Asymptotic x-ray scattering from highly mismatched epitaxial films

2006 J. Phys.: Condens. Matter 18 5047

(http://iopscience.iop.org/0953-8984/18/22/005)

INSTITUTE OF PHYSICS PUBLISHING JOURNAL OF PHYSICS: CONDENSED MATTER

J. Phys.: Condens. Matter **18** (2006) 5047–5055 doi:10.1088/0953-8984/18/22/005

Asymptotic x-ray scattering from highly mismatched epitaxial films

V M Kaganer[1], A Shalimov[2], J Bak-Misiuk[2] and K H Ploog[1]

[1] Paul-Drude-Institut für Festkörperelektronik, Hausvogteiplatz 5-7, 10117 Berlin, Germany
[2] Institute of Physics, Polish Academy of Sciences, aleja Lotników 32/46, 02-668 Warsaw, Poland

E-mail: kaganer@pdi-berlin.de

Received 17 January 2006
Published 16 May 2006
Online at stacks.iop.org/JPhysCM/18/5047

Abstract

We study x-ray diffraction peak profiles from highly mismatched relaxed epitaxial films at momentum transfers exceeding the peak widths. Calculated profiles for misfit dislocations are compared with triple-crystal diffraction profiles from GaAs/Si(001) epitaxial films. We find that the longitudinal and transverse scans have a common q^{-4} asymptote but approach it differently, so that their profiles are qualitatively different in the experimentally available momentum range. The possible contribution from threading dislocations is estimated.

1. Introduction

X-ray diffraction is a well established tool to study various kinds of crystal lattice imperfections. The lattice defects can be very generally divided into two classes [1]: localized defects (e.g., point defects and their clusters) that cause diffuse scattering around a sharp Bragg peak, and extended defects (e.g., dislocations) that give rise to diffraction peak broadening. While defects of the first class are commonly studied by measuring the diffuse intensity distribution to as large as possible momentum transfers, the diffractometry studies of crystals with dislocations are usually based on a comparison of the full widths at half maximum (FWHMs) of different reflections.

The diffracted intensity in a dislocated crystal at large momentum transfers $\mathbf{q}$ (where $\mathbf{q}$ is the deviation from the nearest Bragg point) is due to scattering in the close vicinity of each dislocation line. The dislocation strain field decays as r^{-1}, where r is the distance from the dislocation line. Then, the differential cross-section of x-ray scattering behaves as q^{-5}. The x-ray diffraction measurements involve integrations over one or more components of the momentum transfer $q = |\mathbf{q}|$ resulting in different power laws. In triple-crystal diffractometry, the angular spectrum of the waves scattered by the sample is analysed. An analyser crystal is used, providing a high resolution in the scattering plane. The vertical (normal to the scattering plane) divergence of the scattered waves is not severely restricted, which gives rise to an integration over one component of the three-dimensional vector $\mathbf{q}$ and results in the

q^{-4} dependence. In double-crystal diffractometry, a wide range of waves scattered by the sample is collected by the detector. Since x-ray diffraction is an elastic scattering process, the wavevectors of all scattered waves end at a common sphere (the Ewald sphere), so that an integration over two components of the vector $\mathbf{q}$ is performed, resulting in the q^{-3} law. A similar integration is realized in a powder diffraction experiment, due to the summation of intensities scattered by differently oriented crystallites. The same q^{-3} law, albeit with a different prefactor depending on the diffraction geometry, is realized [1–3]. The q^{-3} law has been experimentally verified in powder diffraction studies of metals [4, 5]. Measurements on single crystalline GaN epitaxial films with large densities of threading dislocations show both q^{-3} and q^{-4} laws, depending on the diffraction mode, double or triple crystal, respectively [6].

X-ray scattering at large momentum transfers originates from the sample regions close to each dislocation line. It follows the universal asymptotic laws described above because of the universal ($\propto r^{-1}$) decay of the dislocation strain. The scattering from all dislocation lines is added up, and the scattered intensity in the asymptotic region is proportional to the total length of the dislocation lines in the sample. Here, we do not consider the higher-order corrections to these power laws that originate from the dislocation correlations [3, 4]. Krivoglaz noted that a measurement in the asymptotic region would be the most straightforward way to obtain the dislocation density (see [1]), but in his time the available x-ray equipment was insufficient for such a kind of experiments. Nowadays, ordinary laboratory x-ray diffractometers allow us to perform such studies.

The aim of the present work is to study the profiles of x-ray diffraction peaks from highly mismatched epitaxial films at momentum transfers q larger than the FWHMs of the peaks. This asymptotic scattering was studied in powders [3–5] and in only one epitaxial system, GaN films with a high threading dislocation density [6]. Our intention is to evaluate the asymptotic scattering from a heteroepitaxial system with misfit dislocations. We show that the approach proposed earlier to calculate diffraction peak profiles from misfit dislocations [7] can be directly extended to the asymptotic region. We also estimate the effects that can arise from correlations between dislocation positions, and an additional contribution from threading dislocations. We compare our calculations to measurements on GaAs/Si(001) films. The films contain, after rapid thermal annealing, periodic arrays of edge misfit dislocations coexisting with random 60° dislocations [8, 9]. The periodic dislocation array is not visible in our study, since it causes non-uniform distortions only in a very narrow range close to the interface [10]. We find that the observed diffraction peaks are well described, being due to a line density $\rho_{\mathrm{M}} = 3.2 \times 10^5$ cm^{-1} of random 60° misfit dislocations.

2. Theory

The x-ray intensity scattered from an epitaxial film disturbed by crystal lattice defects can be represented in the kinematical approximation as

$$I(\mathbf{q}) = \int\int \exp[\mathrm{i}\mathbf{q}\cdot(\mathbf{r}-\mathbf{r}')]\exp[-T(\mathbf{r},\mathbf{r}')]\,\mathrm{d}\mathbf{r}\,\mathrm{d}\mathbf{r}'. \tag{1}$$

Here $\exp[-T(\mathbf{r},\mathbf{r}')]$ is the pair correlation function. In a film, the translational symmetry is broken in the surface normal direction (the distance from the surface to points $\mathbf{r}, \mathbf{r}'$ plays a role) and we cannot write $T(\mathbf{r}-\mathbf{r}')$, as in the case of a uniform infinite system. In strongly distorted crystals, only closely spaced points $\mathbf{r}, \mathbf{r}'$ are correlated and the calculation of the correlation function can be simplified by the approximation of the relative displacements $\mathbf{Q}\cdot[\mathbf{u}(\mathbf{r}) - \mathbf{u}(\mathbf{r}')]$ by distortions $\partial(\mathbf{Q}\cdot\mathbf{u})/\partial\mathbf{r}$ [1]. Here, $\mathbf{Q}$ is the reciprocal lattice vector and $\mathbf{u}(\mathbf{r})$ is the displacement field of a defect.

The calculation of the correlation function for misfit dislocations randomly distributed at the interface between the epitaxial film and the substrate gives [7]

$$T(x,\zeta,z) = w_{xx}(z)x^2 + 2w_{xz}(z)x\zeta + w_{zz}(z)\zeta^2, \tag{2}$$

where x is the distance along the interface between the two points whose correlations are studied, $\zeta = z - z'$ is the distance between these points normal to the surface normal, and z is the coordinate along the surface normal. The coefficients $w_{ij}(z)$ (here $i, j = x, z$) are expressed through integrals over distortions [7]. Here we reproduce only one of them to show the structure of these expressions:

$$w_{xx}(z) = \frac{\rho_{\mathrm{M}}}{2}\int_{-\infty}^{\infty}[Q_x^2(u_{x,x}^{(x)2} + u_{x,x}^{(z)2}) + Q_z^2(u_{z,x}^{(x)2} + u_{z,x}^{(z)2})]\,\mathrm{d}x, \tag{3}$$

where ρ_{M} is the linear density of misfit dislocations, $u_{i,j}^{(x)}(x,z) = \partial u_i^{(x)}/\partial x_j$ are the distortions due to a dislocation with the Burgers vector $\mathbf{b} = (b_x, 0, 0)$ and $u_{i,j}^{(z)}$ are the corresponding distortions for $\mathbf{b} = (0, 0, b_z)$. The calculations are applied to the low-energy dislocations in the zinc-blende structure, namely, the 60° dislocations. Their Burgers vectors make an angle of 60° to the dislocation line directions, so that all misfit dislocations have the same mismatch-releasing component b_x and equal probabilities of the components $\pm b_z$. This ensures the absence of cross-terms in (3).

The analytical formulae for the displacement fields of dislocations lying parallel to a free surface of an elastically isotropic semispace are known (see appendix B in [7]) and the integrals (3) can be evaluated analytically. The resulting expressions are quite bulky and we reproduce only the first term in (3), to show its structure:

$$b_x^{-2}\int_{-\infty}^{\infty} u_{x,x}^{(x)2}\,\mathrm{d}x = \frac{(2-2\alpha+\alpha^2)}{16\pi(d-z)} + \frac{(2-2\alpha+\alpha^2)}{16\pi(d+z)} + \frac{\alpha[(2-\alpha)d^2 - \alpha dz + 2\alpha z^2]}{8\pi d^3} - \frac{dz[(2-\alpha^2)d^2 + 2(2-3\alpha-\alpha^2)dz + (2-6\alpha+5\alpha^2)z^2]}{8\pi(d+z)^5}. \tag{4}$$

Here $\alpha = 1/[2(1-\nu)]$, where ν is the Poisson ratio, d is the film thickness, and the origin $z = 0$ is taken at the free surface. The first two terms in (4) are due to the displacement field of a dislocation in an infinite crystal and its image with respect to the surface, while further terms are due to the surface relaxation term and the cross products. All coefficients $w_{ij}(z)$ in (2) can be represented by analytical expressions similar to (4).

Integration in (1) with the correlation function (2) is performed analytically over x and ζ, since the corresponding integrals are just Fourier transforms of Gaussian functions, which gives

$$I(q_x, q_z) = \int_0^d \frac{\mathrm{d}z}{\sqrt{\det \hat{w}}}\exp\left(-\frac{1}{4}w_{ij}^{-1}q_i q_j\right), \tag{5}$$

where $\hat{w}$ is a 2×2 symmetrical matrix with the elements $w_{ij}(z)$ and w_{ij}^{-1} are the elements of the reciprocal matrix. The diffracted intensity calculations based on equation (5) were performed in [7] with the aim to obtain FWHMs of the peaks. For that purpose, it was sufficiently accurate to replace the $w_{ij}(z)$ by their values at the surface $z = 0$, i.e., take $w_{ij}(0)$ in equation (5). Then, $I(q_x, q_z)$ is an anisotropic Gaussian distribution. This approximation is not suitable for the purposes of the present paper, since our aim is to study the intensity distribution $I(q_x, q_z)$ for q much larger than the FWHM of the peak. Hence, we use equation (5) and perform the integration over z numerically.

Figure 1(a) shows intensity distributions calculated by equation (5) for a symmetric 004 reflection. The misfit dislocation density is taken as $\rho_{\mathrm{M}}d = 64$, to have the same scale as

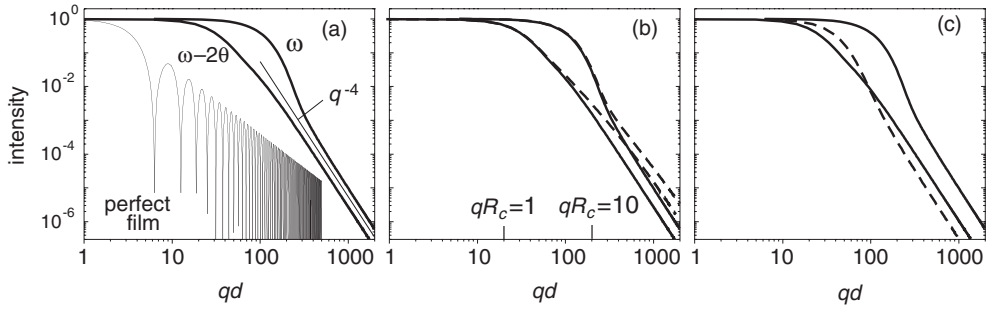

Figure 1. Calculated x-ray diffraction peak profiles of longitudinal (ω–2θ) and transverse (ω) scans for a symmetric 004 reflection. Full lines in (a)–(c) show the curves for uncorrelated misfit dislocations with density $\rho_M d = 64$. The thin line in (a) shows scattering from a perfect film. Dashed lines present (b) correlated misfit dislocations with density $\gamma\rho_M d = 64$ and correlation range $R_c = 0.05d$, and (c) threading dislocations with density $\rho_T d^2 = 4$.

in the experiments presented in the next section. We compare the standard scans of triple-crystal diffractometry, an ω scan (transverse scan, **q** is perpendicular to **Q**) and an ω–2θ scan (longitudinal scan, **q** is along **Q**). The intensity from a perfect film in the longitudinal scan, $I(q) = \sin^2(qd/2)/(qd/2)^2$, is also shown for comparison. Both the longitudinal and the transverse scans from the dislocated film reach the expected q^{-4} asymptotic law for large q. However, this asymptote is reached only after the intensity decreases by at least four orders of magnitude from the peak value. The longitudinal and transverse scans show qualitatively different behaviour in the intermediate q range. In the longitudinal scan, the exponent is smaller than -4 and continuously increases. In contrast, in the transverse scan, the peak is much broader and the intensity decays much steeper in this intermediate q range. The first four orders in intensity are in fact the experimentally available range, so that the pure q^{-4} asymptotic law may not be reached in the experimental scans at all. A notably steeper intensity decrease in the transverse scan for that q range could be erroneously treated as another asymptotic law for the transverse direction. A comparison with the experimental peak profiles in the next section confirms these conclusions.

The calculations above assume a random uniform distribution of uncorrelated misfit dislocations. However, one can expect that the dislocations are positionally correlated to minimize the elastic energy. The positional correlations between dislocations can be described quite easily if the corresponding correlation length R_c is small and $R_c \ll d$ [7]. Then, the correlations can be characterized by a single scalar parameter γ. It is defined through mean square fluctuations of the number of dislocations, $\gamma = \langle(\Delta N)^2\rangle/N$, where N is the number of dislocations in some interval and ΔN is its random variation. Positionally uncorrelated dislocations can be treated as an ideal gas where fluctuations are $\langle(\Delta N)^2\rangle = N$, so that $\gamma = 1$. Positions of correlated dislocations correspond to a liquid, where distances between particles only slightly deviate from the mean distance and $\langle(\Delta N)^2\rangle < N$, so that $\gamma < 1$. We do not consider here the case of periodic dislocations, where it is not sufficient to consider only pair correlations. The effect of pair correlations on the equations above is to replace the true density of misfit dislocations ρ_M by $\gamma\rho_M$. This approximation is valid as long as q is smaller than R_c^{-1}. As q approaches this value, the intensity increases, since the dislocations are effectively less correlated. Hence, the measurement of the diffracted intensity distribution in a wide enough q range allows us to investigate the range of correlations between misfit dislocations.

The effect of pair correlations between dislocations on the correlation function (2) was considered in [7]. In the calculation of the coefficients $w_{ij}(z)$, the square of the distortion in

equation (3), $u^2_{i,j}(x, z)$, has to be replaced by a product of distortions taken at two points x and x', convolved with the correlation function $g(x-x')$. For example, the first term in equation (3) becomes

$$\int \int_{-\infty}^{\infty} u^{(x)}_{x,x}(x, z)u^{(x)}_{x,x}(x', z)g(x - x')\,\mathrm{d}x\,\mathrm{d}x'. \tag{6}$$

More generally, different correlation functions can be introduced for dislocations with one and the same and with different Burgers vectors [7]. If correlations are absent, one has $g(x) = \delta(x)$, where $\delta(x)$ is the delta function. Correlations give rise to $g(x) = \delta(x) - g'(x)$, where the function $g'(x)$ has a characteristic width R_c and possesses the normalization $\int_{-\infty}^{\infty} g'(x)\,\mathrm{d}x = 1 - \gamma$. An effective way to calculate the integral (6) is to perform a Fourier transformation and obtain

$$\int_{-\infty}^{\infty} u^{(x)2}_{x,x}(\kappa, z)g(\kappa)\,\mathrm{d}\kappa. \tag{7}$$

The Fourier transformation of the distortions can be performed analytically; for example, for the distortion component in (7) it is

$$u^{(x)}_{x,x}(\kappa, z) = -\frac{b_x}{2}\left\{[1 - \alpha\kappa(d - z)]\mathrm{e}^{-\kappa(d-z)} + [1 - (2 - \alpha)\kappa d + \alpha\kappa z(2\kappa d - 1)]\mathrm{e}^{-\kappa(d+z)}\right\}. \tag{8}$$

The integral (7) remains to be calculated numerically.

Figure 1(b) shows the effect of the finite correlation range R_c on the the asymptotic scattering. We take $\gamma = 0.16$ and a larger dislocation density, $\rho_M d = 400$, so that the product $\gamma\rho_M d = 64$ remains the same as for uncorrelated dislocations in figure 1(a). The full lines in figure 1(b), coinciding with the ones in figure 1(a), can also be considered as being due to correlated dislocations with values of γ and ρ_M as given above, and with a negligibly small correlation range, $R_c = 0$. To investigate the effect of the finite correlation range, we use an exponential correlation function, $g'(x) = (1 - \gamma)R_c^{-1}\exp(-x/R_c)$, with a correlation length $R_c = 0.05d$. The finite correlation range R_c does not influence the FWHMs of the peaks, since the condition $R_c \ll d$ is satisfied. The asymptotic scattering intensity increases: for $q \gg R_c^{-1}$ it corresponds to uncorrelated misfit dislocations with the linear density ρ_M, to be compared with the effective density $\gamma\rho_M$ that determines the peak width. Hence, for the momentum $q \gg R_c^{-1}$, the scattered intensity is $1/\gamma$ times larger compared with figure 1(a). Thus, the asymptotic scattering can be used to obtain the correlation range R_c for positional correlations of misfit dislocations.

Some misfit dislocations continue as inclined segments that penetrate through the film to the surface. These segments are called threading dislocations. A large density of threading dislocations normal to the surface is typical for GaN epitaxial films. Their effect on the x-ray diffraction peaks can be analysed, similar to the treatment of misfit dislocations above [6]. For III–V semiconductors, threading dislocations degrade the electronic device performance, so that their density should be minimized. An accurate calculation of their effect on the x-ray peaks is much more difficult than for misfit dislocations for several reasons. First, the mean distance between threading dislocations in III–V semiconductors is comparable to or even larger than the film thickness, so that the approximation of the difference of displacements by distortions when calculating the correlation function $T(\mathbf{r}, \mathbf{r}')$ in equation (1) is not valid. Secondly, threading dislocations in III–V semiconductors belong to the same type $\frac{1}{2}\langle 110\rangle\{101\}$ of glide systems as the misfit dislocations. They are 60° dislocations (i.e., the Burgers vectors make an angle of 60° with the dislocation lines) inclined to the surface and are only present as finite segments of the dislocation lines in the film. One needs to calculate the displacement field

of a finite segment of a dislocation line inclined to the surface, which is a fairly complicated elastic problem [11]. So, here we only estimate the effect of the threading dislocations on the diffraction peaks, to compare it with the effect of misfit dislocations.

If the density of threading dislocations ρ_{T} is large enough (the mean distance between dislocations $\rho_{\mathrm{T}}^{-1/2}$ is small compared to the film thickness d), the correlation function $T(\mathbf{r}, \mathbf{r}')$ can be written as (see discussion and references in [6])

$$T(\mathbf{r}, \mathbf{r}') = \frac{(Qb)^2}{4\pi} f \rho_{\mathrm{T}} s^2 \ln\left(\frac{2\pi}{Qb}\frac{L}{s}\right). \tag{9}$$

Here, $s = \left|\mathbf{r} - \mathbf{r}'\right|$ is the distance between points where the correlation is probed and f is a factor of order unity that depends on the relative orientations of all vectors in the problem: the dislocation line direction, the Burgers vector $\mathbf{b}$, the diffraction vector $\mathbf{Q}$, and the vector $\mathbf{r} - \mathbf{r}'$. The calculation of this factor is a difficult task, as discussed above. The distance L is a characteristic screening distance of the dislocation strain fields by either other dislocations or boundaries. For the problem under consideration, it is reasonable to take it equal to the film thickness, $L = d$. The s^2 dependence in (9) gives after Fourier transformation (1) a Gaussian peak profile for q comparable to the FWHM of the peak. The logarithmic term can be approximated by a constant in this range of q. However, in the asymptotic region of large q the logarithmic term provides the power law.

Expression (9) cannot be used for $s > L$. In the numerical Fourier transformation, a rigid upper integration limit causes unphysical oscillations. They can be avoided by replacing L/s in the logarithm of (9) with $(L + s)/s$ [6]. To describe the scattered intensity in the triple crystal diffraction geometry, we integrate (1) over the vertical divergence of the scattered waves and then over the azimuthal angle of the vector $\mathbf{s} = \mathbf{r} - \mathbf{r}'$, assuming f to be constant. Then, the diffracted intensity can be represented by a one-dimensional integral

$$I(q) = \int_0^\infty \exp[-T(s)] J_0(s) s \, \mathrm{d}s, \tag{10}$$

where $J_0(s)$ is the Bessel function. Figure 1(c) presents with a dashed line the peak profile calculated by equations (9) and (10) for a threading dislocation density $\rho_{\mathrm{T}} d^2 = 4$. We expect a rather isotropic intensity distribution after averaging over all relevant dislocation glide systems, so that we set the orientation factor in equation (9) to $f = 1$. Accordingly, only one curve is shown in figure 1(c). The same q^{-4} asymptotic law as for misfit dislocations is obtained. The slope at intermediate q is somewhat in between those for longitudinal and transverse scans of misfit dislocations. Figure 1(c) shows that misfit and threading dislocations have similar effects on the diffraction peak profiles, so that it may be difficult to distinguish them. In the analysis of the experimental profiles below, we therefore decide in favour of misfit dislocations, based on a perfect fit of the FWHMs of both longitudinal and transverse scans in various asymmetric reflections by equation (5).

The threading dislocation density ρ_{T} is a density per unit area, defined as the total length of the dislocation lines per unit volume or, equivalently, a number of dislocation lines crossing a unit area in the plane perpendicular to the lines. The misfit dislocation density ρ_{M} is a density per unit length, defined as a total length of dislocation lines per unit area of the interface or, equivalently, a number of dislocations crossing a line along the interface perpendicular the dislocations. The dimensionless quantities to be compared by their effects on the diffraction peak width are $\rho_{\mathrm{T}} d^2$ and $\rho_{\mathrm{M}} d$. One may need to use $\gamma \rho_{\mathrm{M}} d$ instead of the latter quantity to take into account correlations between misfit dislocations. The effect of correlations between threading dislocations is estimated by the screening length L in (9). We note that, for misfit dislocations, the strain field screening is already provided by the surface elastic relaxation

terms, see for example equation (8). Hence, an approximation of the screening length L for threading dislocations by the film thickness d seems reasonable.

3. Experimental results and discussion

We have studied 2 μm thick GaAs epitaxial films grown by molecular beam epitaxy on vicinal Si(001) [8, 9]. X-ray measurements were carried out with a high-resolution Philips X'Pert Material Research Diffractometer using a four-bounce asymmetric Ge(220) monochromator, a three-bounce Ge(220) analyser, and Cu Kα_1 radiation. We have studied a series of samples with miscut directions [110] and [1$\bar{1}$0] and miscut angles varying from 0.5° to 7.5°. The diffraction measurements performed both along and perpendicular to the miscut direction did not reveal any dependence of the measured curves on the miscut angle or orientation. Hence, the antiphase domains inherent to the GaAs/Si(001) system [12] do not influence the diffraction peaks. The measurement of the diffraction peak positions in symmetric 004 and asymmetric 224 reflections confirms that the GaAs films are fully relaxed, due to a 4% lattice mismatch to the substrate.

The transmission electron microscopy (TEM) measurements [9] showed that, after rapid thermal annealing of the sample, the major part of the mismatch is released by a periodic network of edge misfit dislocations. Periodic edge dislocations coexist with random 60° dislocations, with the density of 60° dislocations found to be from 3% to 11% in the samples investigated by TEM. A periodic dislocation array produces nonuniform strain only in a layer with a thickness smaller than the distance between dislocations [10]. With a dislocation distance of 9 nm, the thickness of this disturbed layer is negligible compared to the GaAs film thickness of 2 μm. Hence, the scattering that we study is due to random 60° misfit dislocations. The TEM measurements also reveal threading dislocations with a density $\rho_T = 2 \times 10^8$ cm^{-2}, so that the dimensionless density $\rho_T d^2 = 8$.

Figures 2(a) and (b) present with bold grey lines longitudinal (ω–2θ) and transverse (ω) x-ray diffraction scans of different symmetric and asymmetric reflections. Diffraction satellites due to a periodic network of edge misfit dislocations are not seen, although their positions would have to be within the q-range of figures 2(a) and (b): with a network period of $p = 9$ nm, the first satellite was located at $qd = (2\pi/p)d = 700$. The satellites are not detected in our measurements since their intensity is too low. Figure 2(c) shows that the effect of the instrumental resolution is negligible: the widths of the 004 diffraction peaks from a perfect Si crystal in transverse and longitudinal scans are 50 and 5.4 times, respectively, smaller than the ones from the GaAs film. We present the instrumental peaks separately since they are not visible in the scale of figures 2(a) and (b).

The observed peaks are fitted to the model of uncorrelated 60° misfit dislocations described above by using just one fit parameter, their density ρ_M. The thin lines in figures 2(a) and (b) are calculated by using equation (5) with one and the same value $\rho_M d = 64$ for all reflections and all scans. The experimental background intensity is added to equation (5). In this way, we can also use for example the 117 reflection, where the dynamical range of available intensities is relatively small and the asymptote is not evident from the plot. The FWHMs of all peaks are fitted very well. We conclude that the random misfit dislocations are the main source of the peak broadening. Their linear density is $\rho_M = 64/d = 3.2 \times 10^5$ cm^{-1}. If we assume that the remaining mismatch is released by periodic edge dislocations, we obtain the fraction of random 60° dislocations as 26% of the total misfit dislocation density. Here we take into account that the Burgers vector component in the interfacial plane is two times larger for edge dislocations. This fraction is larger than the fraction of 60° dislocations obtained by TEM [9]. Our study of

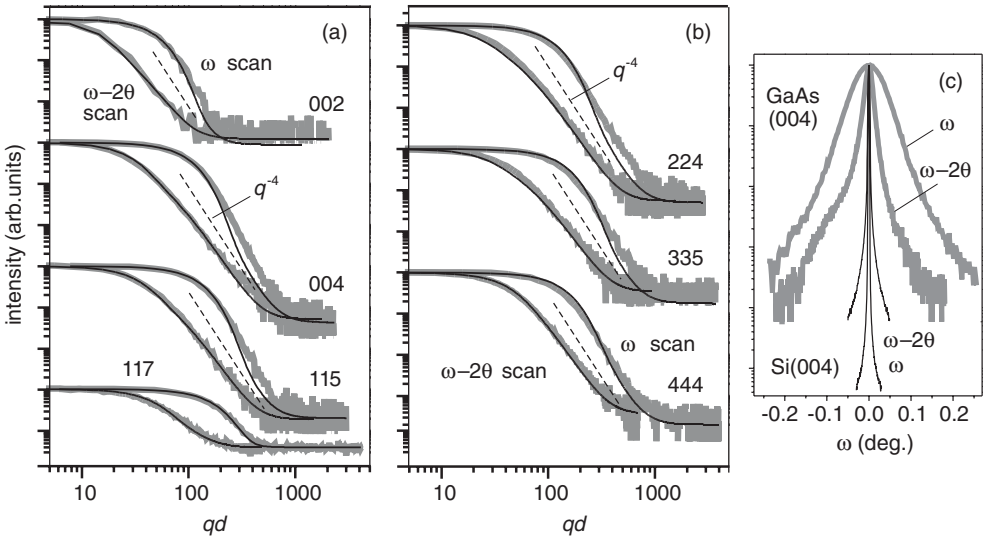

Figure 2. ((a), (b)) Triple crystal x-ray diffraction peak profiles from GaAs/Si(001) epitaxial films (thick grey lines) and calculated profiles (thin black lines) in longitudinal and transverse scans of different reflections and (c) comparison of the peak profiles in 004 reflection from the film (thick grey lines) and from an ideal Si crystal (thin black lines).

FWHMs of the x-ray diffraction peaks on a series of the GaAs/Si(001) samples, to be presented elsewhere, shows that the fraction of 60° dislocations varies in different samples from 9% to 26%, in an agreement with the TEM results.

All longitudinal scans are fitted well in the whole measured q range, spanning more than four orders of magnitude in intensity. Hence, if the 60° dislocations are correlated on small distances, the correlation length R_c for positional correlations should be very small. The intensity distributions follow the q^{-4} asymptotic law up to at least $qd \sim 400$, which gives an estimate for the upper bound $R_c < (2\pi/400)d \approx 30$ nm, which coincides with the mean distance between misfit dislocations $1/\rho_M \approx 30$ nm. This means that the 60° dislocations are not correlated.

The q dependence of intensity in transverse scans is steeper than q^{-4}. This behaviour agrees with the profiles calculated for misfit dislocations in figure 1(a). However, a quantitative comparison in figure 2 shows that the observed intensity is larger than the calculated one in the asymptotic region. The deviations are most pronounced in the 004, 115, and 224 reflections. This additional intensity cannot be attributed to the finite range of positional correlations between misfit dislocations. We have seen in figure 1(b) that such an effect would cause an equal intensity increase in both longitudinal and transverse scans. Threading dislocations also seem improbable as a source of this additional intensity, since they would cause additional broadening of the diffraction peaks with different ratios of FWHMs in the longitudinal and transverse scans. The peak FWHMs in all reflections and all scans could not be fitted together, as is done for the misfit dislocations alone. However, since an accurate quantitative description of the threading dislocations is not yet done, an univocal conclusion about the effect of threading dislocations cannot be reached at this time. The model developed above predicts a steeper intensity decay in the transverse scan than the one observed, which may be the result of the approximations made. In particular, the approximation of elastic isotropy for the dislocation distortion field may not be sufficient.

4. Conclusions

X-ray scattering from dislocation strain fields gives rise (in a triple-crystal diffraction geometry) to an asymptotic q^{-4} law for scattered intensity at large momentum transfers q. Misfit dislocations reveal this asymptote when the intensity decreases by four orders of magnitude from the peak value. In the intermediate q range, the intensities in longitudinal and transverse scans behave differently. In the longitudinal scans, the exponent continuously increases and finally reaches the value -4. The transverse scans show a steeper slope in the intermediate q range. Positional correlations between misfit dislocations result in narrower peaks, while the finite range of their correlations result in an intensity increase in the asymptotic q region. The effect of threading dislocations on the diffraction peak profiles is qualitatively similar to the effect of misfit dislocations. A quantitative description of their contribution, however, seems to be a notably more complicated problem.

We compare the calculated profiles with measurements on GaAs/Si(001) epitaxial films. We find that the FWHMs of both longitudinal and transverse scans in different symmetric and asymmetric reflections can be fitted by the model of random uncorrelated 60° misfit dislocations, and obtain the linear dislocation density $\rho_{\mathrm{M}} = 3.2 \times 10^5$ cm^{-1} from the fit. The longitudinal scans in all reflections are perfectly described by the model of misfit dislocations in the whole measured range of q. This allows us to conclude that the 60° misfit dislocations are not correlated even on small distances. In transverse scans, a steeper intensity decay is observed, in agreement with the calculations. Experimental intensities exceeding the calculated ones in the asymptotic region of the transverse scan possibly point to limitations of the model. We conclude that the effect of threading dislocations on the diffraction peaks is negligible, since they generally lead to different FWHM ratios than the misfit dislocations. Thus, x-ray diffraction peak profiles from relaxed highly mismatched epitaxial films provide much more detailed information on dislocation distributions than just peak widths.

Acknowledgments

We thank A Georgiaklilas for sample preparation and M Calamiotou for fruitful discussions. This work was partially supported by the European Community programme G1MA–CT–2002–4017 (Centre of Excellence CEPHEUS) and by the Polish Committee for Scientific Research under grant No P03B11528.

References

[1] Krivoglaz M A 1996 *X-Ray and Neutron Diffraction in Nonideal Crystals* (Berlin: Springer)
[2] Wilkens M 1963 *Phys. Status Solidi* **3** 1718
[3] Groma I 1998 *Phys. Rev.* B **57** 7535
[4] Groma I 2000 *J. Appl. Crystallogr.* **33** 1329
[5] Székely F, Groma I and Lendvai J 2000 *Phys. Rev.* B **62** 3093
[6] Kaganer V M, Brandt O, Trampert A and Ploog K H 2005 *Phys. Rev.* B **72** 045423
[7] Kaganer V M, Köhler R, Schmidbauer M, Opitz R and Jenichen B 1997 *Phys. Rev.* B **55** 1793
[8] Georgakilas A, Panayotatos P, Stoemenos J, Mourrain J L and Christou A 1992 *J. Appl. Phys.* **71** 2679
[9] Georgakilas A and Christou A 1994 *J. Appl. Phys.* **76** 7332
[10] Satapathy D K, Kaganer V M, Jenichen B, Braun W, Däweritz L and Ploog K H 2005 *Phys. Rev.* B **72** 155303
[11] Indenbom V L and Lothe J (ed) 1992 *Elastic Strain Fields and Dislocation Mobility* (Amsterdam: North-Holland)
[12] Ueda O, Jimbo T S T and Umeno M 1989 *Appl. Phys. Lett.* **55** 445